

Unsupervised MRI Super-Resolution Using Deep External Learning and Guided Residual Dense Network with Multimodal Image Priors

Yutaro Iwamoto¹, Kyohei Takeda², Yinhao Li², Akihiko Shiino³, Yen-Wei Chen¹

¹ College of Information Science and Engineering, Ritsumeikan University, Shiga, Japan

² Graduate School of Information Science and Engineering, Ritsumeikan University, Shiga, Japan

³ Molecular Neuroscience Research Center, Shiga University of Medical Science, Shiga, Japan
yiwamoto@fc.ritsumei.ac.jp

Abstract. Deep learning techniques have led to state-of-the-art single image super-resolution (SISR) with natural images. Pairs of high-resolution (HR) and low-resolution (LR) images are used to train the deep learning model (mapping function). These techniques have also been applied to medical image super-resolution (SR). Compared with natural images, medical images have several unique characteristics. First, there are no HR images for training in real clinical applications because of the limitations of imaging systems and clinical requirements. Second, other modal HR images are available (e.g., HR T1-weighted images are available for enhancing LR T2-weighted images). In this paper, we propose an unsupervised SISR technique based on simple prior knowledge of the human anatomy; this technique does not require HR images for training. Furthermore, we present a guided residual dense network, which incorporates a residual dense network with a guided deep convolutional neural network for enhancing the resolution of LR images by referring to different HR images of the same subject. Experiments on a publicly available brain MRI database showed that our proposed method achieves better performance than the state-of-the-art methods.

Keywords: Super-resolution, Deep Learning, Unsupervised Learning

1 Introduction

Magnetic resonance imaging (MRI) with superior tissue contrast can be employed to visualize detailed internal information of the human body. Multiple MRI sequences (or multimodal MR images) with different tissue contrast such as T1-weighted images (T1WI) and T2-weighted images (T2WI) have been used for accurate medical image diagnosis and analysis tasks such as medical image segmentation [1-3]. The acquisition times of MRI sequences are different—for e.g., a long time is required for T2WI and a short time, for T1WI. Since it is difficult to acquire a high-resolution (HR) image for time-consuming sequences, the resolution of T2WI is usually lower than that of T1WI. Therefore, in the multiple MRI sequences acquired for accurate diagnosis and analysis, the resolution of low-resolution (LR) MRI sequences (e.g., T2WI) should be aligned to

Y. Iwamoto and K. Takeda contributed equally to this work.

the resolution to the HR MRI sequences (e.g., T1WI). Classical interpolation techniques suffer from the problem of image blurring and jaggy artifacts in the interpolated image. In recent years, single image super-resolution (SISR) [4-22] has gained attention as a resolution-enhancement technique. SISR enhances the resolution based on the relationship between the HR and LR images and prior knowledge of various image characteristics. More recently, deep convolutional neural network (CNN)-based SISR methods have been frequently reported in the field of super-resolution (SR) for natural images [4-8] and medical imaging [13-16]. Recently, the number of layers used in these methods was increased, and residual [23] and dense [24] structures were employed to prevent overfitting. In medical imaging, three-dimensional (3D) CNN-based SR are proposed to consider the 3D structure of the volume [14-16]. In addition, the generative adversarial network generates more realistic images by correcting SR images [6, 15]. Thus, the network structure has become more complex, and the number of parameters has increased. Some SR technologies are also proposed for enhancing multimodal images, such as the HR panchromatic images and LR multispectral images in remote sensing [20], HR color images and LR depth images in the consumer depth cameras [21, 22], and MRI sequences in medical imaging [17-19]. Unfortunately, these promising methods [4-7, 14-16] adopt a supervised approach in which many HR images are required. However, in real clinical applications, it is generally difficult to prepare HR medical images because of hardware limitations and clinical requirements.

A few unsupervised approaches [8-13] have been proposed for SISR without HR images for training, and they are based on the self-similarity with the input LR image itself. These approaches can be divided into two groups. The first group [8-10] assumes self-similarity—that is, similar patches are found across identical and different scales within an image itself, and this group is termed “zero-shot” super resolution (ZSSR) [8]. The test LR image is used as an HR image for training, and its simulated degradation image is used as an LR image for training. Such self-training data is called as internal training data in contrast to the external training data (the training data are only used for training). Such learning is called internal learning [8]. In contrast to internal learning, learning based on external training data is called external learning. The limitation of internal learning methods is that a model has to be trained for each test data. Therefore, only simple models (8 hidden layers [8]) are used, and state-of-the-art SR architectures pose a challenge from the viewpoint of computational time of training. Note that the existing methods [8-10] are proposed for natural images. In the second group of methods [11-13], in-plane (x-y plane) images of 3D medical imaging are used as HR images, and their simulated degradation images are used as LR images for training. These methods are used to enhance the resolution along the z-axis.

Motivated by ZSSR, we propose a new unsupervised multimodal guided method for the SR of LR MR images (e.g., T2WI) based on the guidance of HR MR images (e.g., T1WI). The main contributions are summarized below:

- (1) The proposed method uses prepared external LR images as HR images and their simulated degradation images as LR images in the form of external learning. It assumes the simple prior knowledge that the anatomical structures of humans are identical. In unsupervised SR of medical imaging, external learning can achieve better performance compared to internal learning.

- (2) We proposed an HR T1WI guided residual dense network for the resolution enhancement of LR T2WI. By concatenating the multimodal priors (features of HR T1WI) with the features of LR T2WI, we can improve the SR reconstruction accuracy of T2WI in both supervised and unsupervised SR.

2 Proposed Method

2.1 Overview

Figure 1 shows an overview of the proposed method. The method is based on two main concepts. The first one is the use of external LR training images to train the model. The conventional unsupervised approach trains a model using only a test LR image (internal learning) as shown in Fig. 1 (a). Therefore, the method cannot separate the training and test phases, and high computational time (including both training and testing) is required. In addition, since deep learning requires numerous training samples for parameter optimization, excessive data augmentation is used to increase the number of training samples from a single LR image. In the proposed method, we propose to use external LR samples for training as shown in Fig.1(b). These images can be easily collected even in real clinical applications. By using external training LR samples, we can separate the training and test phases. Therefore, a lot of time can be spent for training in advance for using the state-of-the-art SISR framework, and a sufficient number of training samples can be prepared without excessive data augmentation. The second concept is to incorporate multimodal priors (T1WI) into the unsupervised SR framework to guide the resolution enhancement of T2WI as shown in Fig.1(b). In unsupervised learning, since the network is trained in the LR domain, there is a lack of high-frequency components. By using HR guidance images, we can enhance the high-frequency information of the test LR image efficiently.

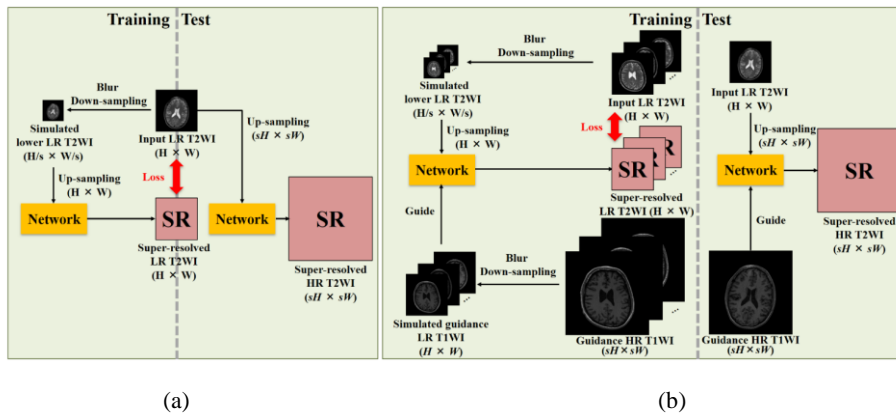


Fig.1. Unsupervised multimodal guided single image super-resolution (SISR) framework. (a) Conventional internal learning-based unsupervised method. (b) The proposed unsupervised method (external learning + guidance by multimodal priors)

2.2 Network architecture

Fig.2 shows the proposed network architecture. The proposed model is inspired by the residual dense network (RDN) [7], which is the state-of-the-art network for various computer vision tasks such as SR. Note that the proposed framework can be combined with a wide variety of existing network architectures as the backbone to further enhance their performance. The model comprises residual and dense structures. The residual network [23] uses shortcut connections, which skip one or more layers. The feature maps are connected by a summing operation. The dense network [24] uses dense connections from any layer to all subsequent layers. The connection is a concatenated operation. The RDN architecture is constructed by some densely connected blocks, and the shortcut connection is arranged on the outside of each dense connection block. The input of the network is an interpolated LR MRI sequence image (e.g., T2WI). The residual training [5] is realized by a shortcut connection from the input to the end of the final layer. In the proposed method, we add a new branch to incorporate the guided HR T1WI as shown in Fig. 2. The features extracted from the guided HR T1WI (multimodal priors) are concatenated with the features of the target T2WI in newly proposed guided residual dense (GRD) blocks as shown in Fig. 2. Each convolutional layer involves 3×3 convolution, batch normalization (BN) [25], and rectified linear unit (ReLU) [26].

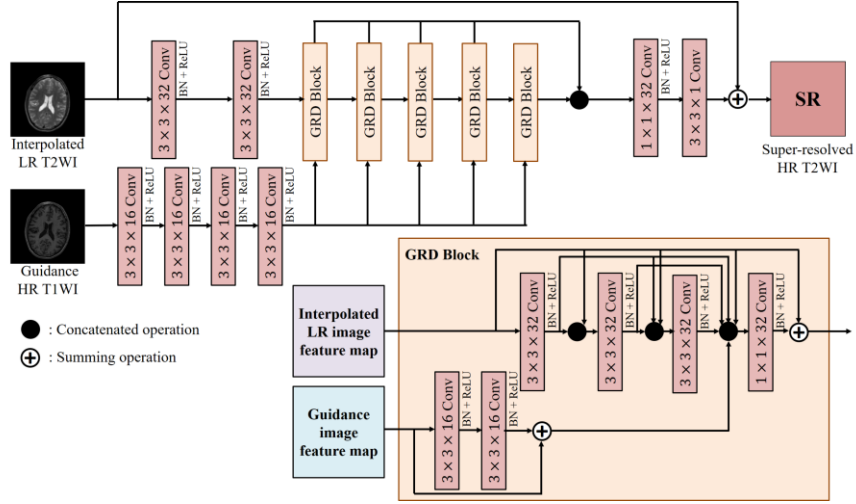


Fig. 2. Network architecture of the proposed method for the resolution enhancement of LR T2WI guided by multimodal priors (HR T1WI).

2.3 Loss function

In the conventional supervised SISR, the basic loss [4] is formulated as follows:

$$L_{supervised}(\Theta) = \frac{1}{N} \sum_{i=1}^N \|f(D^T Y_{Tr}^i; \Theta) - X_{Tr}^i\|_p^p, \quad (1)$$

where Θ is the parameters of CNN; N the number of training samples; $f(\cdot)$, a mapping function (network output); p , a p-norm (SRCNN[4] uses $p=2$); D^T , an up-sampling

operator; \mathbf{Y}_{Tr}^i , an i -th training LR image (e.g., T2WI), and \mathbf{X}_{Tr}^i , the corresponding i -th training HR image (using external HR images). The guided SR includes the corresponding i -th training HR guidance image \mathbf{X}_{TrG}^i (e.g., T1WI) to the network as follows:

$$L_{supervised_guide}(\Theta) = \frac{1}{N} \sum_{i=1}^N \|f(D^T \mathbf{Y}_{Tr}^i, \mathbf{X}_{TrG}^i; \Theta) - \mathbf{X}_{Tr}^i\|_p^p, \quad (2)$$

On the other hand, unsupervised SISR such as ZSSR [8] cannot use training HR images. Therefore, ZSSR uses test LR image \mathbf{Y}_{Te}^i as the HR image and its simulated degradation as LR image $DB\mathbf{Y}_{Te}^i$ (using internal LR training image) as follows:

$$L_{zssr}(\Theta) = \frac{1}{M} \sum_{i=1}^M \|f(D^T DB\mathbf{Y}_{Te}^i; \Theta) - \mathbf{Y}_{Te}^i\|_p^p, \quad (3)$$

where B is a blurring operator; D , a down-sampling operator; and M , the number of training samples (data augmentation using test LR image itself). In the proposed method, we used the external LR images \mathbf{Y}_{Tr}^i as HR images and its simulated degradation images as LR images $DB\mathbf{Y}_{Tr}^i$ (using external LR training images) with training degraded guidance images $DB\mathbf{X}_{TrG}^i$ as follows:

$$L_{unsupervised_guide}(\Theta) = \frac{1}{N} \sum_{i=1}^N \|f(D^T DB\mathbf{Y}_{Tr}^i, DB\mathbf{X}_{TrG}^i; \Theta) - \mathbf{Y}_{Tr}^i\|_p^p, \quad (4)$$

In the test phase, we use the trained network for estimating HR image $\hat{\mathbf{X}}_{Te}$ with HR guidance image \mathbf{X}_{TeG} as follows:

$$\hat{\mathbf{X}}_{Te} = f(D^T \mathbf{Y}_{Te}, \mathbf{X}_{TeG}; \Theta) \quad (5)$$

2.4 Cascade SR strategy and post-processing

In unsupervised approaches (internal learning or external learning), in particular, when the magnification factor is larger, the simulated degradation LR images largely lose their image features, and the ambiguity increases, thereby causing difficulties in estimation. Therefore, to obtain better SR results, we gradually increased the resolution with r stage intermediate magnification scale $\sqrt[r]{s}$ for a the magnification factor s (e.g., when the magnification scale $s = 2$ and the number of stage $r = 3$, the enlarged size from input size ($H \times W$) are stage1: $\sqrt[3]{2}H \times \sqrt[3]{2}W$, stage2: $\sqrt[3]{2^2}H \times \sqrt[3]{2^2}W$ and stage3: $2H \times 2W$). In this experiment, we set r to 3. This idea also used in other self-similarity-based SISR methods [8-10] for natural images to improve the image quality. It also helps to prepare the training dataset by setting a small intermediate magnification factor. Although the methods retrain the network using intermediate estimated SR images, the quality of the final SR image is not guaranteed because of accumulated errors in the intermediate estimated images. On the other hand, our proposed method can correct the estimated SR image based on the HR guidance image of each intermediate step. Thus, the errors can be avoided by adopting guided SR.

In post-processing, we used the iterative back projection (IBP) method [10, 27] to guarantee consistency by minimizing the errors between the estimated SR image projected onto the LR image space and input LR image. IBP is calculated by

$$\mathbf{X}_{t+1} = \mathbf{X}_t + B^T D^T (\mathbf{Y} - DB\mathbf{X}_t), \quad (6)$$

where \mathbf{X}_t is the estimated HR image after the t -th iteration; \mathbf{Y} , the observed LR image; D , the down-sampling operator; D^T , the up-sampling operator. Further, B and B^T are the blurring operators.

3 Experiments

3.1 Data preparation and training parameters

We used NAMIC brain multimodality dataset [28], which includes 20 cases of publicly available brain MRI. The dataset has been acquired using a 3T GE at Brigham and Women’s Hospital in Boston, MA, USA. The voxel dimensions of T1WI (TR = 7.4 ms, TE = 3 ms) and T2WI (TR = 2500 ms, TE = 80 ms) are $1 \times 1 \times 1 \text{ mm}^3$. The matrix size of both images is $256 \times 256 \times 176$. The dataset has already been registered. In this experiment, we used T1WI as the HR guidance image and T2WI as the LR image. To evaluate the SR performance, we generated LR T2WI, which is down-sampled with scaling factors 2 and 4 in the axial plane after Gaussian filtering with sigma set as $s/2\sqrt{2 \ln 2}$ (the full width at half maximum equal to selected slice width [29]). Although we can apply the SR method for volume with slice-by-slice processing, self-similarity-based SR methods such as ZSSR require large computational time with training in the test. Thus, the center slices of each case are evaluated quantitatively with the peak signal-to-noise ratio (PSNR) and structural similarity (SSIM) [30].

We implemented all our models in TensorFlow [31] on a workstation with NVIDIA GeForce GTX 1080 Ti GPU (11GB memory). We used L_1 loss ($p = 1$) with an Adam optimizer [32]. The initial learning rate was set to 10^{-3} , and the rate was divided by 10 if the loss did not continuously reduce over 10 steps. We stopped the training when the learning rate became less than 10^{-6} . Other 3D models [14-16] were reimplemented by two-dimensional (2D) models from 3D convolutional layers to 2D ones (e.g., from $3 \times 3 \times 3$ to 3×3) in this evaluation. For data augmentation, we generated images by rotating 0, 90, 180, and 270 degrees, and flipping horizontally in supervised methods. In addition, we rotated images at 15- and 30- degree intervals, flipping horizontally, and rescaling to reduce the resolution from scaling factors 0.5-1.0 at intervals of 0.1 and 0.2 in ZSSR and unsupervised methods (Ours2, 3 and 4). Here, we used four-fold cross-validation to evaluate our methods. We used the cascade SR strategy by setting r to 3 for both scaling factor $2\times$ and $4\times$ in the unsupervised SISR (Table 2), and we applied a Gaussian filter as an intermediate blurring operator. Here, its standard deviation was set to $\sqrt[3]{s}/2\sqrt{2\lambda \ln 2}$, where λ was set to 2 based on experiments.

3.2 Results

Figure 3 shows the results from different methods for one subject with a magnification factor of 4. The combinations of the proposed method are listed in Table 1 and 2: supervised SISR (external HR images), unsupervised SISR (internal LR image and external LR images) and the existence of the HR guidance image. The results showed that ours1 method obtained the best performance when we used external HR images as the ideal case (supervised learning). Especially, the PSNR of proposed supervised guided method (ours1) achieved better performance compared with the Pham et al. method (10 layers) [16], which obtained the second-highest PSNR value (Table 1). Thus, we demonstrated that the proposed guided network performs better than the state-of-the-

art SR methods, including guided SR methods. When we cannot use the external HR images as real clinical applications (unsupervised learning), ours4 achieved the best performance by a large margin (Table 2). We showed that the strategy using external LR images is more effective than the strategy using internal LR image from a comparison between ZSSR [8] and ours2, ours3 and ours4 (Table 2). This allows us to take advantage of the anatomical similarity between different subjects. In addition, the methods with HR guidance images can recover the detailed structure shown in Fig. 3 (g), (h), and (j) compared with the methods without HR guidance images shown in Fig. 3 (c), (d), (e), (f) and (i) in the red rectangle. The methods using HR guidance images can obtain much higher PSNR values compared to the methods without it.

Table 1. Quantitative evaluation with PSNR and SSIM [30] in the supervised learning using external HR training images.

Method	Guide	2x		4x	
		PSNR	SSIM	PSNR	SSIM
Bicubic interpolation		34.55	0.961	29.62	0.872
SRCNN [4]		38.15	0.981	31.58	0.918
2D DCSRN [14]		38.66	0.984	31.73	0.922
2D mDCSRN – GAN (b4u4) [15]		38.55	0.983	31.69	0.921
2D Pham et al. (10L-ReCNN) [16]	✓	40.93	0.989	35.31	0.964
Ours1	✓	41.48	0.990	36.04	0.969

Table 2. Quantitative evaluation with PSNR and SSIM [30] in the unsupervised learning using internal LR training images or external LR training images.

Method	Internal LR	External LR	Guide	2x		4x	
				PSNR	SSIM	PSNR	SSIM
ZSSR [8]	✓			37.97	0.982	30.71	0.908
Ours2		✓		38.94	0.984	32.10	0.928
Ours3	✓		✓	39.13	0.985	32.60	0.943
Ours4		✓	✓	39.90	0.987	34.39	0.957

4 Conclusion

We introduced a novel external-learning-based unsupervised multimodal priors guided SISR for the resolution enhancement of MRI images (T2WI). Our proposed method can directly utilize accumulated enormous medical image resources at the daily clinical site. In addition, for the proposed method, HR training images for SR do not need to be prepared; thus, this method can be applied to various modalities of medical imaging, which is difficult to acquire HR images for training. Besides, we demonstrated the effectiveness of guided SR guided by multimodal priors (HR T1WI) for recovering the detailed anatomical structure and its advantages over the state-of-the-art method. In future work, we aim to tackle the challenge of building an accurate and efficient unsupervised 3D model.

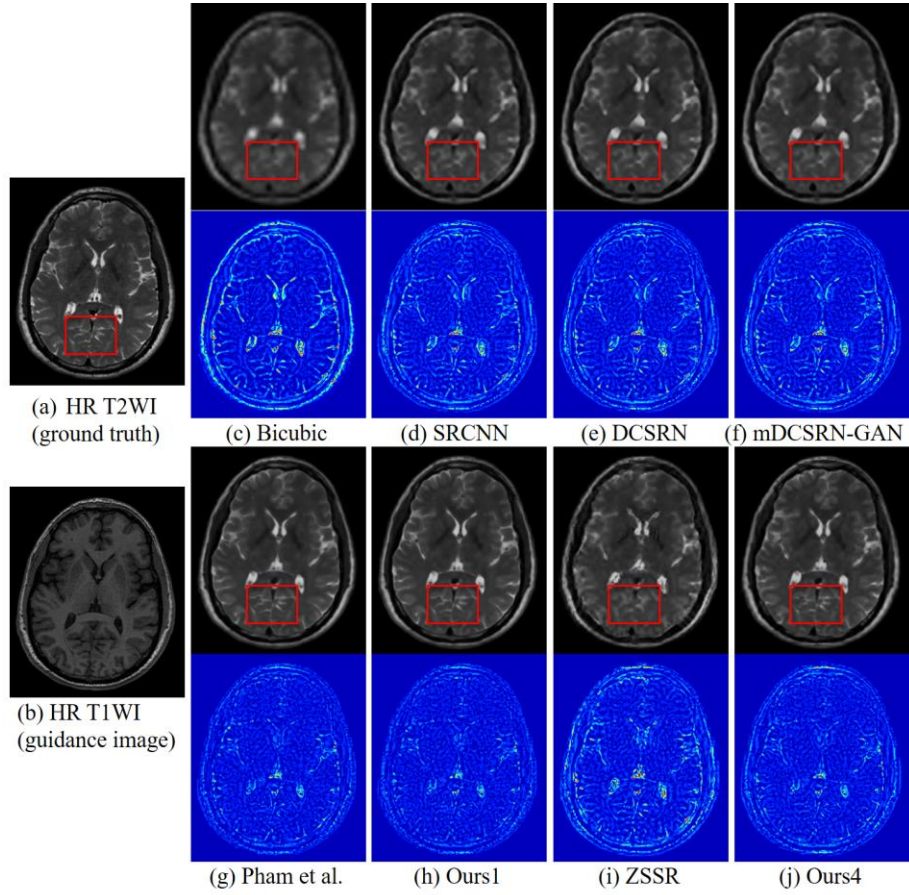


Fig. 3. Visualization of experimental results (up) and the difference between target HR T2WI and each result (down) with magnification factor of 4. (a) Target HR T2WI (ground truth), (b) HR T1WI (guidance image), (c) Bicubic interpolation, (d) SRCNN [4], (e) 2D DCSRN [14], (f) 2D mDCSRN – GAN (b4u4) [15], (g) 2D Pham et al. (10L-ReCNN) [16], (h) Ours 1 (supervised + guide), (i) ZSSR [8], (j) Ours 4 (unsupervised external-learning + guide).

Acknowledgement

This work was supported by JSPS KAKENHI Grant Number 18K18078. The authors would like to thank Enago (www.enago.jp) for the English language review.

References

1. Gordillo, N., Montseny, E. and Sobrevilla, P.: State of the art survey on MRI brain tumor segmentation. *Magnetic Resonance Imaging*, 31(8), 1426-1438 (2013).
2. García-Lorenzo, D., Francis, S., Narayanan, S., Arnold, D.L. and Collins, D.L.: Review of automatic segmentation methods of multiple sclerosis white matter lesions on conventional magnetic resonance imaging. *Medical Image Analysis*, 17(1), 1-18 (2013).
3. Despotović, I., Goossens, B. and Philips, W.: MRI Segmentation of the Human Brain: Challenges, Methods, and Applications. *Computational and Mathematical Methods in Medicine*, 2015(450341), 1-23 (2015).
4. Dong, C., Loy, C.C., He, K. and Tang, X.: Image Super-Resolution Using Deep Convolutional Networks. *IEEE Transaction on Pattern Analysis and Machine Intelligence*, 38(2), 295-307 (2015).
5. Kim, J., Lee, J. K. and Lee, K. M.: Accurate Image Super-Resolution Using Very Deep Convolutional Networks. In: *Proceedings of the IEEE Conference on Computer Vision and Pattern Recognition*, 1646-1654 (2016).
6. Ledig, C., Theis, L., Huszár, F., Caballero, J., Cunningham, A., Acosta, A., Aitken, A., Tejani, A., Totz, J., Wang, Z. and Shi, W.: Photo-Realistic Single Image Super-Resolution Using a Generative Adversarial Network. In: *Proceedings of the IEEE Conference on Computer Vision and Pattern Recognition*, 4681-4690 (2017).
7. Zhang, Y., Tian, Y., Kong, Y., Zhong, B. and Fu, Y.: Residual Dense Network for Image Super-Resolution. In: *Proceedings of the IEEE Conference on Computer Vision and Pattern Recognition*, 2472-2481 (2018).
8. Shocher, A., Cohen, N. and Irani, M.: "Zero-Shot" Super-Resolution Using Deep Internal Learning. In: *Proceedings of the IEEE Conference on Computer Vision and Pattern Recognition*, 3118-3126 (2018).
9. Glasner, D., Bagon, S. and Irani, M.: Super-Resolution Form a Single Image. In: *Proceedings of the IEEE 12th International Conference on Computer Vision*, 349-356 (2009).
10. Timofte, R., Rothe, R. and Gool, L. V.: Seven ways to improve example-based single image super resolution. In: *Proceedings of the IEEE Conference on Computer Vision and Pattern Recognition*, 1865-1873 (2016).
11. Iwamoto, Y., Han, X.H., Sasatani, S., Taniguchi, K., Xiong, W. and Chen, Y.W.: Super-Resolution of MR Volumetric Images Using Sparse Representation and Self-Similarity. In: *Proceedings of the 21st International Conference on Pattern Recognition*, 3758-3761 (2012).
12. Jog, A., Carass, A. and Prince J.L.: Self Super-Resolution for Magnetic Resonance Images. In: *International Conference on Medical Image Computing and Computer-Assisted Intervention*, 553-560 (2016).
13. Zhao, C., Carass, A., Dewey, B.E. and Prince J.L.: Self Super-Resolution for Magnetic Resonance Images Using Deep Networks. In: *2018 IEEE 15th International Symposium on Biomedical Imaging*, 365-368 (2018).
14. Chen, Y., Xie, Y., Zhou, Z., Shi, F., Christodoulou, A.G. and Li, D.: Brain MRI Super Resolution Using 3D Deep Densely Connected Neural Networks. In: *2018 IEEE 15th International Symposium on Biomedical Imaging*, 739-742 (2018).
15. Chen, Y., Shi, F., Christodoulou, A.G., Xie, Y., Zhou, Z. and Li D.: Efficient and Accurate MRI Super-Resolution Using a Generative Adversarial Network and 3D Multi-Level Densely Connected Network. In: *International Conference on Medical Image Computing and Computer-Assisted Intervention*, 91-99 (2018).

16. Pham, C.H., Tor-Díez, C., Meunier, H., Bednarek, N., Fablet, R., Passat, N. and Rousseau, F.: Multiscale brain MRI super-resolution using deep 3D convolutional networks. *Computerized Medical Imaging and Graphics*, 77(101647), 1-15 (2019).
17. Rousseau, F.: A non-local approach for image super-resolution using intermodality priors. *Medical Image Analysis*, 14(4), 594-605 (2010).
18. Manjón, J.V., Coupé, P., Buades, A., Collins, D.L. and Robles, M.: MRI Superresolution Using Self-Similarity and Image Priors. *International Journal of Biomedical Imaging*, 2010(425891), 1-11 (2010).
19. Iwamoto, Y., Han, X.H., Shiino, A. and Chen, Y.W.: Fast super-resolution with iterative-guided back projection for 3D MR images. In: *Proceedings of the SPIE 10574, Medical Imaging 2018: Image Processing*, 105741T (2018).
20. Wei, Y., Yuan, Q., Shen, H. and Zhang, L.: Boosting the Accuracy of Multispectral Image Pansharpening by Learning a Deep Residual Network. *IEEE Geoscience and Remote Sensing Letters*, 14(10), 1795-1799 (2017).
21. Guo, C., Li, C., Guo, J., Cong, R., Fu, H. and Han, P.: Hierarchical Features Driven Residual Learning for Depth Map Super-Resolution. *IEEE Transactions on Image Processing*, 28(5), 2545-2557 (2019).
22. Takeda, K., Iwamoto, Y., and Chen, Y.W.: Color Guided Depth Map Super-Resolution based on a Deep Self-Learning Approach. In: *IEEE Conference on Consumer Electronics*, 2020.
23. He, K., Zhang, X., Ren, S. and Sun, J.: Deep Residual Learning for Image Recognition. In: *Proceedings of the IEEE Conference on Computer Vision and Pattern Recognition*, 770-778 (2016).
24. Huang, G., Liu, Z., Maaten, L.V.D. and Weinberger, K.Q.: Densely Connected Convolutional Networks. In: *Proceedings of the IEEE Conference on Computer Vision and Pattern Recognition*, 4700-4708 (2017).
25. Ioffe, S. and Szegedy, C.: Batch Normalization: Accelerating Deep Network Training by Reducing Internal Covariate Shift. In: *Proceedings of the International Conference on Machine Learning*. 448-456 (2015).
26. Glorot, X., Bordes, A. and Bengio, Y.: Deep Sparse Rectifier Neural Networks. In *Proceedings of the International Conference on Artificial Intelligence and Statistics*, 315-323 (2011).
27. Irani, M. and Peleg, S.: Improving Resolution by Image Registration. *CVGIP: Graphical models and image processing*, 53(3), 231-239 (1991).
28. NAMIC: Brain Multimodality dataset, <http://hdl.handle.net/1926/1687>, last accessed 2020/3/4.
29. Greenspan, H., Oz, G., Kiryati, N. and Peled, S.: MRI inter-slice reconstruction using super-resolution, *Magnetic resonance imaging*, 20(5), 437-446 (2002).
30. Wang, Z., Bovik, A.C., Sheikh, H.R. and Simoncelli, E.P.: Image Quality Assessment: From Error Visibility to Structural Similarity. *IEEE Transactions on Image Processing*, 13(4), 600-612 (2004).
31. Abadi, M., Agarwal, A., Barham, P., Brevdo, E., Chen, Z., Citro, C., Corrado, G.S., Davis, A., Dean, J., Devin, M., Ghemawat, S., Goodfellow, I., Harp, A., Irving, G., Isard, M., Jozefowicz, R., Jia, Y., Kaiser, L., Kudlur, M., Levenberg, J., Mané, D., Schuster, M., Monga, R., Moore, S., Murray, D., Olah, C., Shlens, J., Steiner, B., Sutskever, I., Talwar, K., Tucker, P., Vanhoucke, V., Vasudevan, V., Viégas, F., Vinyals, O., Warden, P., Wattenberg, M., Wicke, M., Yu, Y. and Zheng, X.: TensorFlow: Large-Scale Machine Learning on Heterogeneous Distributed Systems. 2015. Software available from tensorflow.org.
32. Kingma, D.P. and Ba, J.L.: Adam: A Method for Stochastic Optimization. In *International Conference on Learning Representations*, 2015.